

Effects from A-site substitution on morphotropic phase boundary and phonon modes of $(\text{Pb}_{1-1.5x}\text{La}_x)(\text{Zr}_{0.42}\text{Sn}_{0.40}\text{Ti}_{0.18})\text{O}_3$ ceramics by temperature dependent Raman spectroscopy

X. Chen, Z. G. Hu, Z. H. Duan, X. F. Chen, G. S. Wang, X. L. Dong, and J. H. Chu

Citation: *Journal of Applied Physics* **114**, 043507 (2013); doi: 10.1063/1.4816093

View online: <http://dx.doi.org/10.1063/1.4816093>

View Table of Contents: <http://scitation.aip.org/content/aip/journal/jap/114/4?ver=pdfcov>

Published by the [AIP Publishing](#)



Goodfellow

metals • ceramics • polymers
composites • compounds • glasses

Save 5% • Buy online
70,000 products • Fast shipping

Effects from A-site substitution on morphotropic phase boundary and phonon modes of $(\text{Pb}_{1-1.5x}\text{La}_x)(\text{Zr}_{0.42}\text{Sn}_{0.40}\text{Ti}_{0.18})\text{O}_3$ ceramics by temperature dependent Raman spectroscopy

X. Chen (陈啸),¹ Z. G. Hu (胡志高),^{1,a)} Z. H. Duan (段志华),¹ X. F. Chen (陈学锋),²
 G. S. Wang (王根水),² X. L. Dong (董显林),² and J. H. Chu (褚君浩)¹

¹Key Laboratory of Polar Materials and Devices, Ministry of Education, Department of Electronic Engineering, East China Normal University, Shanghai 200241, China

²Key Laboratory of Inorganic Functional Materials and Devices, Shanghai Institute of Ceramics, Chinese Academy of Sciences, Shanghai 200050, China

(Received 7 April 2013; accepted 3 July 2013; published online 23 July 2013)

The complex perovskite ferroelectric/antiferroelectric of $(\text{Pb}_{1-1.5x}\text{La}_x)(\text{Zr}_{0.42}\text{Sn}_{0.40}\text{Ti}_{0.18})\text{O}_3$ (PLZST) ceramics have been investigated by Raman scattering spectra from 77 to 480 K. It was found that phase transition occurs between La composition of 2.6% and 2.8% for PLZST ceramics. Softening of $A_1(\text{TO}_1)$ mode and dramatic changes of relative strength from $E(\text{TO}_2)$ mode are observed at morphotropic phase boundary (MPB). Moreover, it was found that MPB characteristic shows a wider and lower trend of temperature region with increasing La composition. This could be ascribed to the diminishment of the energy barrier and increment of A-cation entropy.
 © 2013 AIP Publishing LLC. [<http://dx.doi.org/10.1063/1.4816093>]

I. INTRODUCTION

In the past few decades, the complex Pb-based ABO_3 perovskite materials have attracted much attentions due to the excellent properties (ferroelectric, antiferroelectric, piezoelectric, and pyroelectric) obtained in the compositions close to morphotropic phase boundary (MPB).¹⁻⁸ This issue is intensively studied in the PbZrO_3 - PbTiO_3 (PZT) system for two boundaries, which are approximately located at 5% and 52% of Ti portion. Note that the former boundary separates the antiferroelectric (AFE) and ferroelectric (FE) phase. Moreover, incorporation of Sn^{4+} in the B-cation, for the pseudoternary PbZrO_3 - PbTiO_3 - PbSnO_3 (PZST) system, can enhance the stability of the AFE region. The Ti portion in antiferroelectric PZST can be increased up to 10%, which makes PZST much easier in compositional tailoring. It results in some uniquely physical properties and technique applications by the doping/substitution engineering.

Plenty of researches are focused on the B cation variation, in both macroscopic properties and microstructure.³⁻⁶ However, recent studies have shown anomalistic macroscopic properties induced by the A-site substitution. For example, Chan *et al.*⁸ reported the electrical properties of La-modified lead zirconate stannate titanate (PLZST) in two different phases, which was induced by La-introduction. It was observed that pure PZST was FE state at room temperature. However, 2% La concentration destabilizes FE state and transforms into an incommensurate AFE state. Further increasing of La composition enhanced the stability of the AFE state at room temperature. Recently, the phase transition from rhombohedral to tetragonal structure is revealed between La compositions of 2.6% and 2.8% with aid of ultraviolet-infrared reflectance spectra.⁹ On the other hand, the temperature of the

electric field induced phase transition at MPB is 120 °C and 45 °C for 2% and 3% La composition, respectively.^{10,11} It indicates that the A-site substitution plays an important role in phase transition and more studies are requisite.¹²

According to the phase diagram of PZST, established by Berlincourt,¹³ and XRD results,¹⁴ PLZST material with different compositions near MPB presents tetragonal and rhombohedral structures, corresponding to AFE and FE phases. Nevertheless, there is no physical consensus on mechanism determining the nature of anomalistic macroscopic properties for PLZST system to date. Compared to the aforementioned macroscopic properties studies, the microstructure of PLZST, especially from the A-site substitution effect is seldom reported. Therefore, more studies on the microstructure changes are necessary to clarify the phase transition process for PLZST materials at MPB. Generally, Raman scattering as a nondestructive characterization technique is sensitive to symmetry disturbance. It could provide some invaluable information of the order-disorder phenomena and lattice vibration corresponding to the symmetry. The scattering spectra of vibration modes in different frequencies could be a crucial and widely used measurement tool for investigating phase transition issue.¹⁵⁻¹⁸ Based on the spectral analysis, the phonon modes can be explained by the variations of frequency, intensity, and full width at half maximum (FWHM).

In this work, the A-site substitution effect on the phase transition near MPB is investigated for PLZST ceramics. Transition temperature region and lattice dynamics are systematically discussed according to the temperature dependent Raman scattering spectroscopy.

II. EXPERIMENTAL DETAILS

The compositions of PLZST investigated in the present work are $(\text{Pb}_{1-1.5x}\text{La}_x)(\text{Zr}_{0.42}\text{Sn}_{0.40}\text{Ti}_{0.18})\text{O}_3$ (100x/42/40/18) wherein, $x = 2\%$, 2.6%, 2.8%, and 3.4% (hereafter denoted

^{a)}Author to whom correspondence should be addressed. Electronic mail: zghu@ee.ecnu.edu.cn. Tel.: +86-21-54345150. FAX: +86-21-54345119.

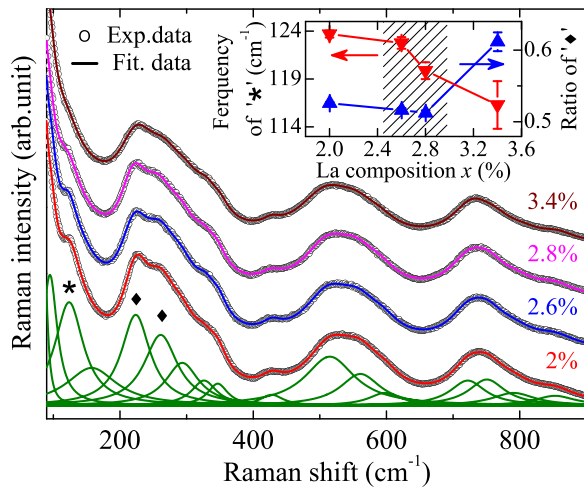


FIG. 1. Raman scattering spectra of $(\text{Pb}_{1-1.5x}\text{La}_x)(\text{Zr}_{0.42}\text{Sn}_{0.40}\text{Ti}_{0.18})\text{O}_3$ ceramics with different La composition recorded at room temperature. The symbols (\star and \blacklozenge) indicate the $A_1(\text{TO}_1)$ mode and $E(\text{TO}_2)$ mode, respectively. The inset shows the frequency variation of $A_1(\text{TO}_1)$ mode (\blacktriangledown) and relative strength of $E(\text{TO}_2)$ mode (\blacktriangle) as a function of La composition. Note that the shadow pattern indicates the MPB region.

as PLZST2, PLZST2.6, PLZST2.8, and PLZST3.4, respectively). The bulk ceramics were fabricated by traditional solid-state ceramic processing route.⁹ The samples were sintered at 1300 °C for 1 h in air atmosphere. Then all samples with the diameter of 15 mm and the thickness of 1 mm were single-side polished for Raman measurements. Temperature dependent Raman spectral experiments were carried out by a Jobin-Yvon LabRAM HR 800 micro-Raman spectrometer and a THMSE 600 heating/cooling stage (Linkam Scientific Instruments) in the temperature range from 77 to 480 K with a resolution of 0.1 K. The ceramics were excited by the 488 nm line of an Ar laser at a power of ~ 20 mW and recorded in back-scattering geometry with a resolution better than 1 cm^{-1} . The laser beam was focused through a $50\times$ microscope with a working distance of 18 mm. An air-cooled charge coupled device (CCD) (-70°C) with a 1024×256 pixels front illuminated chip was used to collect the scattered signal dispersed on 1800 grooves/mm grating.¹⁶ In order to learn more about the variation trend of vibration modes, all of the experimental spectra were fitted with independent damped harmonic oscillators.

III. RESULTS AND DISCUSSION

Fig. 1 depicts room-temperature Raman scattering results and well-fitted deconvolution peaks for all samples.

TABLE I. The assignment of symmetries from the fitting deconvolution peaks in Raman scattering of PLZST ceramics recorded at room temperature. Note that the unit for the phonon modes is cm^{-1} .

Samples	Symmetries														
	$A_1(\text{TO}_1)$	$E(\text{LO}_1)$	$E(\text{TO}_2)$	$E(\text{TO}_2)'$	$E(\text{TO}_3)$	$E(\text{LO}_2)$	$A_1(\text{TO}_2)$	$A_1(\text{LO}_2)$	$E(\text{TO}_4)$	$E(\text{TO}_4)'$	$A_1(\text{TO}_3)$	$E(\text{LO}_3)$	$E(\text{LO}_4)$	$A_1(\text{LO}_3)$	O breathing
PLZST2	124.5	156.2	223.5	261.7	294.2	326.4	347.2	428.0	514.7	561.0	598.8	723.1	751.9	792.1	852.7
PLZST2.6	122.8	160.5	221.3	257.9	290.8	326.0	346.5	428.4	512.3	557.7	593.7	724.7	753.8	793.3	850.9
PLZST2.8	119.9	160.7	220.3	257.3	291.6	325.9	346.0	427.6	511.1	554.9	590.2	722.8	752.6	796.8	852.8
PLZST3.4	116.3	161.6	224.2	265.6	298.8	329.9	350.6	427.3	508.3	554.3	588.8	728.3	762.1	803.9	856.7

Although all of four spectra present similar profiles, two featuring differences could be recognized as the softening of the peak at $\sim 125 \text{ cm}^{-1}$ (labeled as “star”) and the competition of two peaks at $\sim 220 \text{ cm}^{-1}$ and $\sim 260 \text{ cm}^{-1}$ (labeled as “diamonds”). In order to analyze the above featuring differences, assignment of the symmetries is necessary. Nevertheless, the present assignments are according to the results reported from PLZT and PZT due to the lack of theoretical research on the symmetries of PLZST.^{4,18} Note that the phonon mode assignments at room temperature are listed in Table I. It should be emphasized that the assigned modes are necessary in order to reasonably interpret Raman spectra, where some broadening peaks appear.¹⁸ There are two peaks assigned as $E(\text{TO}_2)$ mode, stemming from the T_{1u} mode in the cubic phase. The mode corresponds to the vibrations of B -cation against the oxygen octahedra cage in the plane perpendicular to polarization. The mode is split due to different atoms in the B -site. It was reported that the relative peak area of $E(\text{TO}_2)/[E(\text{TO}_2)+E(\text{TO}_2)']$ ratio, corresponding to the relative strength of split $E(\text{TO}_2)$ modes, changes dramatically when the symmetry is varied through the MPB.⁵ The value in tetragonal phase is much higher than that in rhombohedral phase. A sharp increase of relative strength of $E(\text{TO}_2)$ mode could be observed at La composition of 2.8%, as shown in the inset of Fig. 1. This indicates that PLZST3.4 ceramic is more likely to be tetragonal phase rather than the rhombohedral phase in the PLZST2 ceramic.

The softening peak upon La composition is assigned as $A_1(\text{TO}_1)$ symmetry, which stems from splitting of T_{1u} in cubic phase.⁴ As seen in Fig. 1, it undergoes both suppression in intensity and softening in frequency. Similar suppression of the modes induced by La-doping for $\text{Pb}_{1-x}\text{La}_x\text{Sc}_{(1+x)/2}\text{Ta}_{(1-x)/2}\text{O}_3$ and $\text{Pb}_{1-x}\text{La}_x\text{Sc}_{(1+x)/2}\text{Nb}_{(1-x)/2}\text{O}_3$ single crystals was recently reported by Maier *et al.*¹⁷ The symmetry is considered to consist of displacements of the B -cation and oxygen ions relative to Pb^{2+} ions in PZT and to mark the transition from paraelectric to ferroelectric phase.⁴ The suppression indicates that polar order is disturbed due to the replacement of A -site cation with a smaller ionic radius.¹⁷ This disturbance may result in the antiparallel polar order for AFE phase. Besides, an accurate softening procedure is recognized from the inset of Fig. 1. The mode softs from 123.4 cm^{-1} (PLZST2) to 116.3 cm^{-1} (PLZST3.4) with an incommensurate drop at La composition of 2.6%. The fact that both of two dramatic changes occur indicates the phase transition from rhombohedral to tetragonal structure for La composition between 2.6% and 2.8%, which is in good agreement with previous XRD and reflectance spectra study.⁹

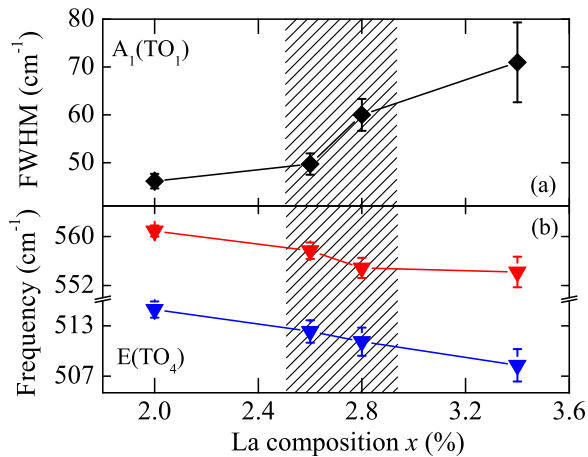


FIG. 2. (a) FWHM variation of $A_1(TO_1)$ mode with La composition. (b) Frequency shift of split $E(TO_4)$ mode as a function of La composition at room temperature. Note that the shadow pattern indicates the MPB region.

The effect of La-doping could also be recognized in the FWHM of the $A_1(TO_1)$ mode, which is corresponding to the damping of oscillators. As seen in Fig. 2(a), the FWHM value increases with increasing La composition, indicating the enhanced anharmonicity of the vibrations and disorder of the system.¹⁹ A sharp increase could be observed between La composition of 2.6% and 2.8%. Fig. 2(b) presents the shift towards lower frequency of split $E(TO_4)$ mode. The $E(TO_4)$ mode stems from the T_{1u} mode in the cubic phase, arising from the internal BO_6 bending modes.⁴ Similar to the $E(TO_2)$ mode, the split is considered as the chemical disorder of B -site cations. The peak shift indicates that the strength of average B -O interactions becomes weaker with the La doping.¹⁷ Due to the substitution of La^{3+} cation for Pb^{2+} cation, oxygen atoms without one positive charge inside the octahedra will repel each other more for charge compensation. This effect gives rise to the weakness of the bond, which may also result in the disorder of the perovskite oxide system.

Next, let us concern temperature dependent Raman spectra of four PLZST ceramics. For example, Fig. 3 presents the spectra recorded at several characteristic temperatures. Note that all four samples should be located the paraelectric phase at 480 K. Similar to the PLZT,¹⁸ there are three main bands, locating at $\sim 250\text{ cm}^{-1}$, $\sim 500\text{ cm}^{-1}$, and $\sim 750\text{ cm}^{-1}$, respectively. On cooling, the bands from

four samples present a shift to higher frequency. One of the contributions to the shift is thermal expansion of lattice.¹⁹ The other contribution is considered as soft mode effect, especially for the low wavenumber region. An interesting feature is the splitting of the band at $\sim 250\text{ cm}^{-1}$ on cooling (labeled as “diamond”). Moreover, the splitting temperature decreases with increasing La composition. As for PLZST3.4 ceramic, the splitting is not obvious even at 77 K, as compared to the other samples. Moreover, the $A_1(TO_1)$ mode (labeled as “star”), only presents as a small shoulder for PLZST3.4, which is also quite distinct from the recognizable peaks in other ceramics. The two featuring variations with the temperature indicate that La-doping plays an important role in lattice dynamic of PLZST ceramics.

In order to distinguish two different phases across the MPB, the temperature dependent relative strength of split $E(TO_2)$ mode is plot in Fig. 4. The value should be much larger in tetragonal phase than that in rhombohedral phase.⁵ The dramatic variation region of the relative strength indicates the symmetry change near the MPB. As shown in Fig. 4, the values of relative strength for four compositions are up to 0.9 at high temperature and down to 0.3 at low temperature, respectively. The anomalies at 200 K could arise from the doubling of the unit cell in low temperature.²⁰ It is quite clear that the region is wider and shifts to low temperature as increasing La composition. Another significant information is that the $A_1(TO_1)$ mode is onset of softening in the low-temperature-side boundary of shadow region and sharply soft to a lower wavenumber in the region. As for PLZST3.4, however, the determination of the region is slightly obscure because the relative strength of $E(TO_2)$ mode (above 0.6) in the rhombohedral side is higher than that of other ceramics (under 0.6). It was reported that revealing the exact transition temperature and width of perovskite oxides is still difficult from electrical measurements, even in the intensively studied paraelectric to ferroelectric phase transition, where only the maximum of dielectric response is detected.²¹ From Fig. 4, the phase transition widths of the PLZST ceramics can be roughly estimated to 50 K, 65 K, 100 K, and 150 K, corresponding to increasing La composition. These values are slightly larger than those for $Pb_{0.5}Sr_{0.5}TiO_3$ films derived from refractive index.²¹ Nevertheless, the temperatures, at which the maximum of broad dielectric peak appears, are located

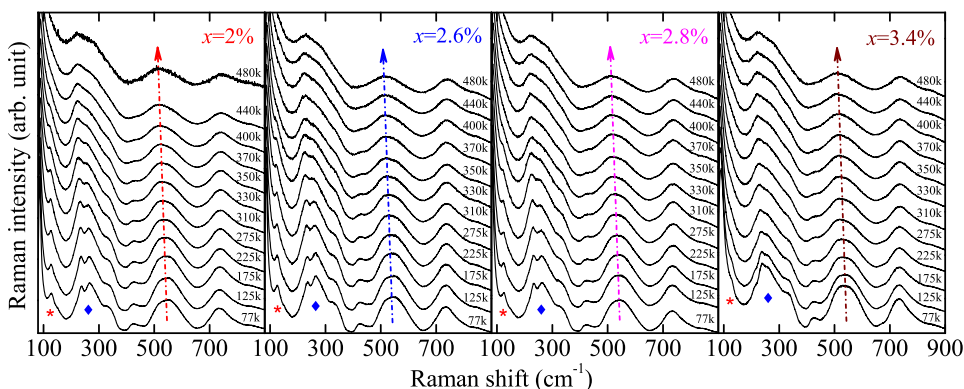


FIG. 3. Temperature dependence of Raman spectra for $(Pb_{1-1.5x}La_x)(Zr_{0.42}Sn_{0.40}Ti_{0.18})O_3$ ceramics from 77 to 480 K. The symbols ($*$ and \blacklozenge) indicate the $A_1(TO_1)$ mode and $E(TO_2)$ mode, respectively. The dash lines are applied to guide the eyes.

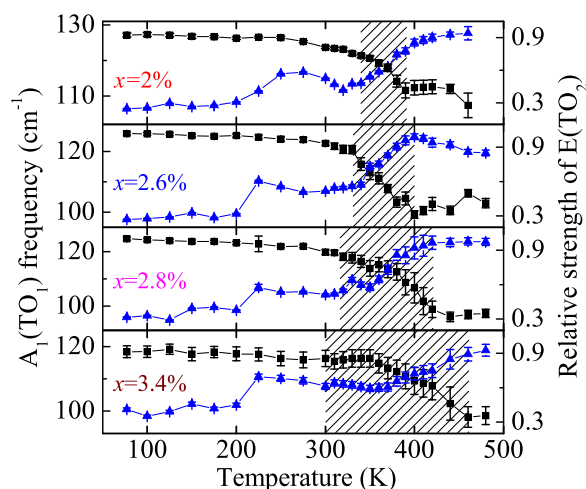


FIG. 4. Temperature dependence of $A_1(\text{TO}_1)$ mode frequency (■) and relative strength of $E(\text{TO}_2)$ mode (▲) for $(\text{Pb}_{1-1.5x}\text{La}_x)(\text{Zr}_{0.42}\text{Sn}_{0.40}\text{Ti}_{0.18})\text{O}_3$ ceramics. Note that the shadow pattern indicates the MPB region, which is different with increasing La composition.

in the width regions.¹⁰ Note that the present data are derived by combining the variations from relative strength of split $E(\text{TO}_2)$ mode with $A_1(\text{TO}_1)$ mode frequency. On the other hand, the frequency of $A_1(\text{TO}_1)$ mode at 77 K (under 120 cm^{-1}) is lower than that of the other three (above 125 cm^{-1}). This effect could arise from the anharmonicity of the vibrations and disorder of the system, which was confirmed by increasing FWHM of $A_1(\text{TO}_1)$ mode.

From the aforementioned discussion, softening procedure of $A_1(\text{TO}_1)$ mode, relative strength change of $E(\text{TO}_2)$ mode and enhanced anharmonicity of the vibrations and disorder in the system indicate that the A -site substitution can induce phase transition near MPB, which takes place at La-composition of 2.6% and 2.8%. The influence of La-doping on the transition from ferroelectric-rhombohedral phase to antiferroelectric-tetragonal phase could be understood by the Goldschmidt tolerance factor (t) framework, where systematic structural octahedral tilt transition may be expected. The tilt transition could induce significant changes in the ferroelectric phase behavior. Because the ionic radius of La^{3+} (1.36 \AA) is smaller than that of Pb^{2+} (1.49 \AA), the parameter t decreases with increasing La composition in the A -site, which indicates that more AFE phase may be observed.²² Besides, it is well known that the ABO_3 perovskite structure is a three-dimensional network of regular corner-linked BO_6 octahedra with small B cations at the center of each octahedron and larger A cations being centrally located in the AO_{12} cuboctahedral cavity formed by eight octahedra. The A -site substitution with different ionic radius could induce a local elastic field and the pressure induced phase transition near the MPB was reported by Ahart *et al.*² This could be another plausible reason for La-induced phase transition near the MPB. Second, there is more space in the cuboctahedral cavity because of smaller ionic radius of La^{3+} . This would increase the entropy of the A -site cation, which means a decrease of the transition temperature.²³ In

addition, B -site cations trend to displace in different directions. As a consequence of the competition on displacement, the ratio of the lattice constants c/a should be small, which has been conformed by previous report.⁹ This means that the distortion of tetragonal is not far from that of rhombohedral. The coexistence of the two phases should be considerable, as indicated by the above phase transition width (Fig. 4). It was reported that the increment of La amount diminishes the energy barrier, which separates free energy minima corresponding to FE and AFE states for PLZT material.²⁴ This results in a wider temperature region for the MPB characteristics with more La composition.

IV. CONCLUSION

In summary, La-doping effect on lattice dynamics of $(\text{Pb}_{1-1.5x}\text{La}_x)(\text{Zr}_{0.42}\text{Sn}_{0.40}\text{Ti}_{0.18})\text{O}_3$ ceramics has been investigated. The room temperature analysis confirmed that La-induced phase transition at morphotropic phase boundary occurs between La composition of 2.6% and 2.8%. The transition region, at which ferroelectric-rhombohedral phase steadily transforms to antiferroelectric-tetragonal, becomes wider and lower in temperature with increasing La composition.

ACKNOWLEDGMENTS

One of the authors (X.C.) would like to thank Jiajun Zhu and Yuanyuan Liao for fruitful discussions. This work was financially supported by Major State Basic Research Development Program of China (Grants Nos. 2011CB922200 and 2013CB922300), Natural Science Foundation of China (Grant Nos. 11074076, 61106122, and 60906046), Projects of Science and Technology Commission of Shanghai Municipality (Grant Nos. 11520701300 and 13JC1402100), and the Program for Professor of Special Appointment (Eastern Scholar) at Shanghai Institutions of Higher Learning.

¹A. S. Mischenko, Q. Zhang, J. F. Scott, R. W. Whatmore, and N. D. Mathur, *Science* **311**, 1270 (2006).

²M. Ahart, M. Somayazulu, R. E. Cohen, P. Ganesh, P. Dera, H. K. Mao, R. J. Hemley, Y. Ren, P. Liermann, and Z. Wu, *Nature (London)* **451**, 545 (2008).

³J. J. Zhu, W. W. Li, G. S. Xu, K. Jiang, Z. G. Hu, M. Zhu, and J. H. Chu, *Appl. Phys. Lett.* **98**, 091913 (2011).

⁴M. Deluca, H. Fukumura, N. Tonari, C. Capianni, N. Hasuike, K. Kisoda, C. Galassi, and H. Harima, *J. Raman Spectrosc.* **42**, 488 (2011).

⁵E. Buixaderas, M. Berta, L. Kozielski, and I. Gregora, *Phase Transitions* **84**, 528 (2011).

⁶Y. Yan, K.-H. Cho, and S. Priya, *Appl. Phys. Lett.* **100**, 132908 (2012).

⁷W. Y. Pan, C. Q. Dam, Q. M. Zhang, and L. E. Cross, *J. Appl. Phys.* **66**, 6014 (1989).

⁸W.-H. Chan, Z. Xu, T. F. Hung, and H. Chen, *J. Appl. Phys.* **96**, 6606 (2004).

⁹X. Chen, K. Jiang, Z. G. Hu, X. F. Chen, G. S. Wang, X. L. Dong, and J. H. Chu, *Appl. Phys. Lett.* **101**, 011914 (2012).

¹⁰H. L. Zhang, X. F. Chen, F. Cao, G. S. Wang, X. L. Dong, Y. Gu, and Y. S. Liu, *Appl. Phys. Lett.* **94**, 252902 (2009).

¹¹H. L. Zhang, X. F. Chen, G. Yu, F. Cao, C. L. Mao, G. S. Wang, X. L. Dong, and Y. L. Wang, *Ferroelectrics* **402**, 150 (2010).

¹²N. N. Luo, Y. Y. Li, Z. G. Xia, and Q. Li, *Cryst. Eng. Comm.* **14**, 4547 (2012).

- ¹³D. Berlincourt, *IEEE Trans. Sonics Ultrason.* **13**, 116 (1966).
- ¹⁴C. T. Blue, J. C. Hicks, S. E. Park, S. Yoshikawa, and L. E. Cross, *Appl. Phys. Lett.* **68**, 2942 (1996).
- ¹⁵W. J. Zhang, W. W. Li, X. G. Chen, Z. G. Hu, W. Liu, G. S. Wang, X. L. Dong, and J. H. Chu, *Appl. Phys. Lett.* **99**, 041902 (2011).
- ¹⁶Y. Y. Liao, Y. W. Li, Z. G. Hu, and J. H. Chu, *Appl. Phys. Lett.* **100**, 071905 (2012).
- ¹⁷B. J. Maier, A. M. Welsch, B. Mihailova, R. J. Angel, J. Zhao, C. Paulmann, J. M. Engel, W. G. Marshall, M. Gospodinov, D. Petrova, and U. Bismayer, *Phys. Rev. B* **83**, 134106 (2011).
- ¹⁸E. Buixaderas, V. Bovtun, S. Veljko, M. Savinov, P. Kužel, I. Gregora, S. Kamba, and I. Reaney, *J. Appl. Phys.* **108**, 104101 (2010).
- ¹⁹I. El-Harrad, C. Carabatos-Nédelec, J. Handerek, Z. Ujma, and D. Dmytrow, *J. Raman Spectrosc.* **25**, 799 (1994).
- ²⁰E. Buixaderas, I. Gregora, S. Kamba, P. Kužel, and I. Reaney, *Appl. Phys. Lett.* **94**, 052903 (2009).
- ²¹M. Tyunina, A. Dejneka, D. Chvostova, J. Levoska, M. Plekh, and L. Jastrabik, *Phys. Rev. B* **86**, 224105 (2012).
- ²²C. J. Cheng, D. Kan, S. H. Lim, W. R. McKenzie, P. R. Munroe, L. G. Salamanca-Riba, R. L. Withers, I. Takeuchi, and V. Nagarajan, *Phys. Rev. B* **80**, 014109 (2009).
- ²³J. Frantti, V. Lantto, and J. Lappalainen, *J. Appl. Phys.* **79**, 1065 (1996).
- ²⁴V. M. Ishchuk, V. N. Baumer, and V. L. Sobolev, *J. Phys.: Condens. Matter* **17**, L177 (2005).